Carbon Dots: Synthesis and Properties

Subjects: Nanoscience & Nanotechnology | Chemistry, Applied
Contributor: Smita Das, Pranab Goswami, Lightson Ngashangva

Carbon dots (CDs) are zero-dimensional optically active carbon-based nanomaterials with a size of less than 10 nm. The material property of the CD is largely linked to the various bottom-up & top-down synthesis approaches, including surface passivation and functionalization, and the carbon precursors. The CDs can be engineered to enhance the chemical and physical functional properties by doping with heteroatom such as nitrogen, phosphorus, sulfur, fluorine, and boron. Because of its various advantageous properties, CDs are utilized in the field of chemical/biological sensing, bioimaging, and drug delivery. These nanosized CDs can change their light emission properties in response to various external stimuli such as pH, temperature, pressure, and light. The CD's remarkable stimuli-responsive smart material properties have recently stimulated massive research interest for their exploitation to develop various sensor platforms.

Keywords: Carbon dots ; Synthesis ; Bioimaging ; Sensor ; Catalyst ; Nanomaterials ; Drug-delivery ; Photoluminescence

1. Introduction

Since the fortuitous discovery of carbon dots (CDs) in 2004, the interest in these luminescent nanomaterials has been increasing exponentially [1][2]. The CDs are quasi-spherical nanomaterials having dimension of less than 10 nm. Compared to the different types of carbon nanomaterials, the CDs have gained enormous attention due to its certain advantages such as inexpensive and easy synthesis, facile surface functionalization, low toxicity, biocompatibility, high water-solubility, tunable luminescence property, and stability at room temperature [3]. Consequently, their applications are explored in bioimaging, drug delivery, and chemical/biological sensing [4]. Additionally, carbon dot's enzyme-like activity has also attracted wide interest because of their potential to replace the naturally occurring enzymes, as the latter is ordinarily unstable, expensive, and challenging to synthesize on a large scale [5].

At present, the concept of employing CDs as smart material is of great interest in material and analytical sciences. A material is termed "smart" when it experiences variation in response to a significant external physical or chemical stimulus that includes light, temperature, pH, solvent, stress, and electric and magnetic field [6]. The synthesis and applications of these smart material or stimulus-responsive materials have been among the principal focus of research in recent times. Such materials can change the outlook of modern science & technology and engineering at large. In this context, CDs have increasingly appealing research interest as potential smart materials for their wide applications in bioanalytical sciences.

2. Synthesis

CDs being the rising star of fluorescent carbon nanoparticles have captivated the interest of the researchers for their application in various fields. Depending on the structure, CDs are classified as graphene quantum dots (GQDs), carbon nanodots (CNDs), and polymer dots (PDs). GQDs have graphene layer/s that can be connected with functional groups. CNDs are spherical shaped, and they can be further divided into carbon nanoparticles and carbon quantum dots based on the crystal lattice. PDs are formed due to aggregation or cross-linking of polymers [7]. Therefore, different CDs may be devised and engineered to obtain the desired property by following various synthetic routes.

Diverse methods for the synthesis of CDs are known. Typically, the synthesis process can be grouped into two: Top-down and bottom-up [8]. The top-down approach usually follows breaking-down/cleaving larger carbon molecules to smaller molecular structures, whereas the bottom-up approach involves building-up/step-wise chemical fusion of small carbon molecules by pyrolysis or carbonization. Some known top-down approaches include electrochemical/chemical oxidation, laser ablation, and ultrasonic treatment, whereas the bottom-up approaches include hydrothermal/solvothermal, microwave-assisted, thermal decomposition, carbonization, pyrolysis, and ultrasonic treatment. Some prominent reports on the synthesis of CDs via these two routes are mentioned in Table 1.

Table 1. Synthesis of carbon dots (CDs) following top-down and bottom-up approach.

Precursors	Synthesis Route/Temp/Time	Types of CDs	Size(nm)/QY (%)	Ref
QR, NaOH	Ultrasonic RT/6 h	CDs	2.99/27.7	[9]
CA, PEG	Ultrasonic RT/1 h	CDs	2.38/NA	[10]
Soybean	Ultrasonic 2 h	NBDs	24/16.7	[11]
Graphite, ethanol	Laser ablation 800 nm, 150 fs	CDs	F_s 1.4/NA $2F_s$ 2/NA F_d-2 1.1/NA F_d-10 1.5/NA	[12]
DEASA, H_3PO_4	Hydrothermal 200 °C/2 h	CDs	4.69/19.4	[13]
Jeera	Hydrothermal 250 °C/6 h	CDs	6–9/5.33	[14]
Tobacco	Hydrothermal 300 °C/3 h	CDs	2.14 ± 0.3/27.9	[15]
Cryptococcus	Hydrothermal 160 °C/1 h	CDs	4–9/14.13	[16]
TMA	Hydrothermal 260 °C/12 h	CDs	4.3/13.4	[17]
Agaricus bisporus	Hydrothermal 160 °C/12 h	CDs	NA/4.2	[18]

Chitosan, AA	Hydrothermal 180 °C/12 h	CQDs	5/NA	[19]
CA, EA	Hydrothermal 180 °C/8 h	CDs	4/NA	[20]
Folic acid, Glucose	Hydrothermal 210 °C/12 h	CDs1 CDs2	1.6/23.5 2.6/42.8	[21]
Xylose, H_3PO_4, m-PD	Microwave 220 °C/10 min	CDs1	6.80/73.6	[22]
Xylose, H_3PO_4, m-PD	Microwave 200 °C/10 min	CDs2	7.23/56.1	
Xylose, H_3PO_4, m-PD	Microwave 180 °C/10 min	CDs3	6.80/40.9	
Xylose, m-PD HNO_3	Microwave 220 °C/10 min	CDs4	9.88/65.3	
Xylose, m-PD CH_3COOH	Microwave 220 °C/10 min	CDs5	8.83/49.5	
Xylose, m-PD	Microwave 220 °C/10 min	CDs6	6.87/42.8	
Xylose, m-PD, Na_3PO_4	Microwave 220 °C/10 min	CDs7	16.37/8	
Xylose, m-PD, NaOH	Microwave 220 °C/10 min	CDs8	10.70/6.8	
CA, EDA	Microwave 720 W/2 min	CDs	4/24	[23]

CA, urea	Microwave 750 W/5 min	CDs	NA/NA	[24]
Anthracite coal, H_2SO_4, HNO_3	Pyrolysis in oil bath 120 °C/24 h	CDs	3.5/NA	[25]
CA, Glu, Asp, lysine	Thermal pyrolysis 200 °C/30 min	CDs	4/8.8	[26]
CA, acrylamide	Solvothermal 200 °C/4 h	CDs	9.5/NA	[27]
CA	Oven 200 °C/1h	CDs	3/NA	[28]

DEASA: 4-(diethylamino) salicylaldehyde; CA: Citric acid; EA: Ethanolamine; AA: Acetic acid; SC: Sodium citrate; QR: quinaldine red; RT: room temperature; PEG: poly(ethylene glycol); NBDs: nano biomass dots; F_s: single-pulse ablation (F_{single} = 50 J·cm^{-2}); $2F_s$: single-pulse ablation ($2F_{single}$); F_d-2: double-pulse ablation (τ_{delay} = 2ps); F_d-10: double-pulse ablation (τ_{delay} = 10 ps); EDA: ethylene diamine; TMA: Trimellitic acid; m-PD: m-phenylenediamine; NA: Not Available.

The different physicochemical properties like the degree of carbonization, crystallinity, size, morphology, and photoluminescence properties are attained depending on the type of synthesis method and the precursor molecule. For instance, the hydrothermal method is less harsh than the pyrolytic method, but the former generally yields incomplete carbonization, molecular fluorophores, amorphous CDs, whereas the latter predominantly yields graphitic core structures. The functional groups like amine, carboxyl, and hydroxyl on the surface of carbon dot can modify the physicochemical properties, biocompatibility, and stability, thus influencing the selectivity, and sensitivity of the CDs in the analytical applications. Additionally, the molecular precursors used for the synthesis of CD influences the degradation process and other environmental behavior [29].

As stated before, various ranges of CD materials with different properties could be achieved by different synthesis conditions. It has been recently observed that if bottom-up synthetic approaches are followed, high PL quantum yield (QY) results. Due to the harsh conditions being applied in the bottom-up synthesis approach, multiple side-products may be produced along with the CDs. Citrazinic acid and other small fluorophore derivatives are produced while synthesizing the nitrogen-doped CDs from citric acid, contributing to the emission in the blue spectral range. Such molecular species and polymerized nanoparticles may attach to the CDs to enhance the optical properties [30][31].

2.1. Heteroatoms Doped-CD Synthesis

The inherent properties of the CDs can be modulated by doping with heteroatoms such as nitrogen (N), phosphorus (P), sulfur (S), boron (B), and fluorine (F), individually or in various combinations during the synthesis. The introduction of the heteroatoms further adds new electronic, chemical, and optical functionalities to the CD, thereby broadening its application. Depending on the type of element, doping is categorized into non-metal and metal doping.

2.1.1. Non-Metal Doping

Nitrogen-doped (N-doped) CDs are the most commonly explored type of non-metal doping because of the closer electronic structure with that of carbon. The N-doped CDs are fabricated by introducing the nitrogen element to the carbon dot core. For the first time in a study, multicolor emissive CDs were synthesized using inorganic ammonium salt via a solvothermal method. The synthesized CDs with increased nitrogen content resulted in high quantum yield of ~4% and led to the introduction of new functional groups like cyano. However, because of the carbon dot's multicolor emissive property,

these CDs have also opened up various applications for sensing and antibacterial activity [32]. The N-doped CDs developed by using *Lantana camara* berries via a simple green approach exhibited good quantum yield (QY) of 33.15%, high stability, high biocompatibility. Additionally, the N-CDs could also detect Pb^{2+} with high sensitivity and selectivity [33]. Red emissive N-doped CDs was synthesised from citric acid and ethylenediamine through a microwave-assisted pyrolysis method. During the synthesis, the effect of the molar ratio of ethylenediamine to citric acid, pyrolysis time, and the concentration of the reactants was taken into consideration. The optimized molar ratio between amine/acid was found to be 0.75 with an exposure time of 88 s in 1100 W microwave power. The fabricated N-doped CDs displayed remarkable biocompatibility and can further be used in bioimaging applications [34]. In most instances, the CDs synthesis with co-doping enhances the properties of the nanomaterial. Interestingly, human fingernails as precursor was used to fabricate N, S co-doped CDs through a simple microwave irradiation procedure that exhibited good stability and a QY of 42.8%. More importantly, the method does not require any passivating agent or a passivation step for the synthesis. The N, S co-doped CDs were employed to detect a synthetic dye, sunset yellow and in cell imaging [35].

2.1.2. Metal Doping

Doping CDs with metal ions can modify the charge density and surface properties, thus effectively tuning the optical features of the nanomaterial. For instance, the Cu-doped CDs exhibited enhanced peroxidase-like activity due to the enhancement of the electronic properties and modification of the surface properties after the introduction of the metal ion [36]. In another study, the developed Cu-doped CDs using ethanediamine and copper chloride dihydrate ($CuCl_2{\cdot}2H_2O$) as precursors possessed notable photostability for up to 60 min. Then again, manganese doped CDs (Mn-CDs) displayed excellent fluorescence QY (>54.4%). By using spectroscopic techniques and DFT-based frontier orbital calculation, it was found that the high QY is due to the change of the oxidation state of Mn from Mn-oxide to Mn-carbonate during the synthesis [37]. Some more examples of metal-doped CDs are given in Table 2 for further reference.

Table 2. Synthesis of heteroatoms doped CDs following top-down and bottom-up approach.

Precursors	Synthesis Route/Temp/Time	Types of CDs	Size (nm)/ QY(%)	Ref
Cryomilled graphite, DMF	Laser ablation 800 °C/3 h	N-CDs	3/4.05	[38]
2-aminopyrimidine-5-boronic acid	Laser ablation 170 mW/1014 Wcm^{-1}	N, B-CD	3/58	[39]
Graphite rods and ammonia hydroxide	Electrochemical and ultrasonic 80 °C/3 h	N-CDs	3–5/NA	[40]
L-tryptophan, chlorhexidine acetate	Hydrothermal 200 °C/12 h	N-CDs	~4.0/NA	[41]
P. acidus, aq. ammonia	Hydrothermal 200 °C/12 h	N-CDs	5/12.5	[42]
PVP	Hydrothermal 200 °C/6 h	N-CDs	6.5/6	[43]

EDA, $CuCl_2.2H_2O$	Hydrothermal 180 °C/10 h	Cu-CDs	1.8/7.8	[44]
Aphen, CA	Hydrothermal 200 °C/7 h	AC-CDs	25/52	[45]
OPD, ABPA	Hydrothermal 160 °C/6 h	B,N-CDs	4.09/8.56	[46]
$Mn(III)(C_5H_7O_2)_3$	Hydrothermal 200 °C/12 h	MnO_x-CDs	5.65 ± 0.30/11.3	[47]
Sucrose, nitrobenzene, nitrosobenzene	Hydrothermal 180°C/12 h	CD-NO, and CD-NO_2	gCD 11/21 rCD 13/18	[48]
CA, EDA	Microwave 300 W/10 min	N-CDs	~5/95, 11	[49]
CA, EDA, sodium borate		B-CDs	~5/63, 9	
CA, EDA, K_2PO_4		P-CDs	~5/63, 6	
p-PDA, EDA	Microwave 500 W/20 min	N-CDs	4.8/14	[50]
TSCDH, Urea, DMF	Solvothermal 160 °C/4 h	$N\text{-}CD_{11}$	4.5/21.6	[51]
TSCDH, Urea, DMAC		$N\text{-}CD_{12}$	4.5/18.7	
TSCDH, Urea, DEF		$N\text{-}CD_{21}$	4.5/17.6	
H_2O_2, ethanol, NH_3	Solvothermal 180 °C/NA	N-CDs	2.15/56.1	[52]
CA, PD	Solvothermal 170 °C/4 h	Y-CDs	7.2/24	[53]
CA and DAN	Solvothermal 160 °C/6 h	HCP-DB-CDs	2.4/70 ± 10	[54]

PAA, CuN, HH, $(NH_4)_2S_2O_8$	Carbonization/polymerization and pyrolyzation Stirring/24 h and 400 °C/90 min	Cu-CDs	2.8/36	[55]
Willow Catkin, Urea and H_2SO_4	Combustion	N,S-CDs	7.3/14.3	[56]
Na_2[Cu(EDTA)] and Ascorbic acid	Thermolysis 250 °C/2 h	Cu-CDs	3.48/9.8	[57]

PAA: Poly(acrylic acid); CA: Citric acid; MA: Melamine; DTSA: Dithiosalicylic acid; EDA: Ethylenediamine; TSCDH: Trisodium citrate dihydrate, DMF: dimethylformamide, DMAC: dimethylacetamide; DEF: dimethylformamide; EA: Ethanolamine; Glu: Glutamic acid; Asp: Aspartic acid; AA: Acetic acid; TNP: 3,4,9,10-tetranitroperylene; PEI: poly(ethyleneimine); p-PDA: p-phenylenediamine; OPD: O-phenylenediamine; ABPA: 3-aminophenylboronic acid; PD: 2,3-phenazinediamine; Aphen: 5-amino-1,10-phenanthroline; Ru-Aphen: 5-amino-1,10-phenanthroline ruthenium (II) complex; AC: ammonium citrate; SBH: sodium borohydride; DAN: diaminonaphthalene; CuN: Copper nitrate; HH: Hydrazine hydrate; DMF: dimethylformamide; NA: Not Available.

2.2. Surface Passivation and Functionalization of CDs

Apart from doping, the intrinsic properties of the CD can be effectively tuned during their synthesis by tailoring the surface chemistry via surface passivation/functionalization. During the process of surface passivation, functional groups like -OH, -COOH, and $-NH_2$ are introduced onto the surface of the CDs, which further enhance the physical property such as solubility and specific chemical reactivity in general as well [58]. In a study, Bai et al. demonstrated that the polydopamine (PDA) passivated CDs exhibited triple times more QY than the original CDs in the absence of PDA and also displayed 1.5 times enhancement of nucleation site for CD formation **[59]**.

The surface functionalization of the CDs with different precursors such as L-cysteine (N, S), ethylenediamine (N), and glycine (N, O) resulted in high fluorescence QY and improved selectivity for different metal ion detection due to different binding abilities [60]. Understanding the interaction between the CD system and the passivating agents is crucial to tailor the CD's fluorescent properties. For example, the synthesis routes influence the CD-polymer nanoparticle system's interaction, that ultimately influencing the photoluminescence property [61]. Ions like Zn^{2+} was also used to develop passivated CDs using zinc gluconate by pyrolysis method of synthesis. The presence of Zn^{2+} during the synthesis prevents the aggregation and improves the stability and optical property of the synthesized CD [62].

The passivation methods and surface functionalization are followed not only to produce better stability and improve the PL intensity but also to enhance other vital characteristics of CDs. Chirality is very important in terms of catalysis, chiral recognition, and even sensing. Recently, Rao and the group developed a strategy using the surface passivation method to prepare chiroptical carbon quantum dots via two steps pyrolytic route. They used tartaric acid and citric acid as carbonaceous sources while producing carbon core, whereas D/L-penicillamine molecules were used to surface passivating agent. In order to retain the chiral information, one of the critical findings of the study was to maintain the reaction temperature lower than the melting point of the ligand in the second pyrolytic step. Interestingly, the strategy did not depend on the chirality of the carbon source [63]. Another interesting study is the effects of surface functionalities of carbon dot during cellular uptakes. Here, the CDs which were passivated with two chemical moieties, 3-ethoxypropylamine (EPA-CDs) and poly(ethyleneimine) (PEI-CDs) were considered to evaluate their uptake mechanism, pathways, and effects in HeLa cells (human cervical carcinoma cells). As expected, the internalization pathways of the two CDs were different in the HeLa cells; however, the efficiency of the internalization process with PEI-CDs was higher in comparison to the EPA-CDs. The different moieties present on the surface of CDs could affect the overall behaviors of CDs uptake [64].

2.3. Characterization of CDs

The unique and typical properties of CDs are exhibited due to their size, shape, chemical skeleton/composition, and structure. So, there have been continuous attempts to explore robust and reliable techniques for their characterization. In this section, some of the updated characterization techniques for CDs are discussed briefly as the characterization of CDs

has been discussed more in recent reviews and chapters [65][66][67].

2.3.1. Microscopic and Diffraction Technique

Non-destructive imaging and microscopic techniques are used to study morphology and different dimension of nanosized particles. Some of the techniques which are being routinely explored for the measurements of CDs are transmission electron microscopy (TEM), scanning electron microscopy (SEM), atomic force microscopy (AFM), X-ray diffraction (XRD).

The morphology, size distribution, or particle size of carbon dots can be investigated using TEM and SEM. These techniques can be used to determine agglomeration or dispersion of the prepared particles as well. SEM technique is employed to investigate if the particle size ranges from 1–20 nm, and in case if the measurement exceeds the resolution of SEM, TEM, which could offer better-resolving power, is more advised. Nowadays, high-resolution TEM (HRTEM) is extensively used to study the structure and crystalline nature. To understand dimensional surface images of CDs, AFM is being used to obtain 2D images and 3D information of the surface morphology and topography of CDs. Depending on their diffraction patterns, crystalline materials can be characterized by XRD. Thus, the particle size, crystal structure, and purity of carbon dots are investigated through this technique. It is a valuable characterization technique to obtain crystallite features, but the technique could also be used to study amorphous CDs [7][68].

2.3.2. Spectroscopic Technique

Spectroscopic techniques can characterize the synthetic features of carbon dots. Some of the commonly used spectroscopic tools are ultraviolet-visible spectroscopy (UV-Vis), Fourier transform infrared spectroscopy (FTIR), nuclear magnetic resonance spectroscopy (NMR), photoluminescence spectroscopy (PL), and Raman spectroscopy.

FTIR determines and identifies the functional groups such as carbonyl (-C=O), amine/amide ($-NH_2$/-CN), hydroxyl (-OH), ether/epoxy (-O-), and others that are present on the surface of the CDs. The presence of moieties and heteroatoms in CDs such as boron (B), nitrogen (N), sulfur (S), silicon (Si), and phosphorus (P) could be identified using such technique. The fine structure information of metal-doped CDs such as aluminium (Al), nickel (Ni), or magnesium (Mg) can be further characterized by X-ray photoelectron spectroscopy [65].

Another important spectroscopic technique is Raman spectroscopy, a non-destructive and non-invasive method to identify the CDs state. Generally, Raman spectra of carbon dots have two first-order bands, i.e., D- and G-band. D bands signify the vibration of carbon atoms of disordered graphite or glassy carbon, whereas the G band represents the vibration of sp^2 carbon atoms. The degree of purity or graphitization of CDs could be estimated by the ratio of D band and G band (D/G). A high D/G ratio indicates the amorphous nature, and a high degree of graphitization gives a relatively lower D/G ratio.

NMR usually employs to understand the structural information of CDs further. The presence of sp^2 carbon, sp^3 carbon, functional groups like -C=O, $-NH_2$, and -OH can be distinguished with the resonance spectroscopy. ^{13}C-NMR could be used to distinguish further and confirm the presence or absence of aliphatic carbon or aromatic carbon on the CDs skeleton. The optical properties of CDs are extensively investigated with the help of UV-Vis and PL spectroscopic techniques. The absorption and the photoluminescence properties of CDs are explained more in the later part of the review.

One of the powerful tools to elucidate the chemical structure of smaller-sized nanoparticles is mass spectrometry (MS). Some of the MS techniques which have been applied and used to characterize CDs are electrospray ionization quadrupole time-of-flight tandem mass spectrometry (ESI-Q-TOF-MS/MS), inductively coupled plasma-mass spectrometry (ICP-MS), and matrix-assisted laser desorption/ionization time-of-flight mass spectrometry (MALDI-TOF-MS) [69][70].

3. Properties

CDs are fascinating nanomaterials with remarkable inherent physical and chemical properties that allow their application in diverse fields. Therefore, an in-depth study and understanding of the CD's optical, physical, and chemical properties are essential to further improve its characteristics in order to broaden its applications.

3.1. Physical Property

3.1.1. Chemical Structure

Carbon dots usually are less than 10 nm with quasi-spherical nano-sized carbon particles. However, as mentioned earlier, synthesis routes dictate the various chemical structure of carbon dots. For instance, GQDs are anisotropic with a crystalline structure of one or more graphene layers. Different analytical techniques such as microscopic, spectroscopic,

spectrometric, and diffraction methods are employed to confirm and ascertain the morphology, functional groups, size distribution, and crystalline nature of CDs. For example, the morphology of microstructure CDs-based lubricants following the ultrasonic approach was studied with TEM and HRTEM and found to be 2.38 nm on average and highly crystalline with 0.21 nm lattice spacing and (100) graphene plane [10]. The structural elucidation of defects and or graphitization could be further confirmed with Raman spectrometry by analyzing the G band and D band. By following the pulsed laser ablation synthesis method, nitrogen-doped GQDs were prepared and obtained a 3 nm particle size by Neon and co-workers. The as-prepared N-GQDs exhibited 1565 cm^{-1} as G band and 1311 cm^{-1} as D band in Raman spectrum, confirming the disordered structure [38]. XRD is a powerful instrument to characterize the physical state of the synthesized carbon dots. The amorphous character of CDs is observed as a broad hump, which is centered in and around ~2θ = 26° in the XRD profile. Nearly spherical amorphous clusters of ~4–18 nm diameters were observed in the self-passivated CDs from dextrose by following the ultrasonication approach [71].

3.2. Chemical and Optical Property

3.2.1. Ultraviolet-Visible Absorption

The basic chemical structure of CDs can be significantly elucidated by the typical UV-vis spectral analysis. The presence of π-π* (C=C) and n-π* (C=O, C-N, C-S, etc.) transition of the CDs skeleton indicates the type of surface functional groups, routes of CD synthesis, precursors, and chemical environment. For example, the absorption bands of CDs at around 273 nm and 342 nm may imply sp^2 hybridization of the π electrons and n-π* transition, respectively [13]. Again, the combination of the same carbon but different nitrogen sources also influences the absorption' bands position [54][72]**.** The presence of heteroatoms (such as N, O, P, B, S, and Se) in the CD's molecular structure also results in the fluctuations of the UV-vis peaks. The N, S-CDs fabricated from 3-aminothiophenol via a one-pot hydrothermal method showed two absorption shoulders at 298 nm, and 354 nm attributed to n-π* transition and heteroatoms N and S surface states defect, respectively [73].

3.2.2. Photoluminescence

The most impressive characteristic feature of CDs is the photoluminescent (PL) or the fluorescent property, which has allowed them to expand their field of applications. The PL of CDs is influenced by surface chemistry, quantum size effect, and molecular states of the carbon core. The up-conversion photoluminescence (UCPL) in the near infrared region carbon dots (NIR-CDs) may be because of the thermally activated electron transition from $S_{1\text{-edge}}$ to $S_{1\text{-Int}}$ in the excited state as shown in Figure 1i [74]. The various synthetic approaches (as shown in Tables 1 and 2) along with different starting materials result in the generation of CDs with unique structures and different luminescent behaviors such as white, blue, green, yellow, red, and deep ultraviolet emission. Since the CDs are fabricated from variable carbon sources via different routes, the PL behavior also depends on the size, solvent, pH, and many more. Generally, due to the diverse electronic transition pathways, the CDs exhibit broad, symmetrical luminescence spectra across the whole wavelength scale. Various energy levels may be created by O-containing groups (named as O-related defect state), P-containing groups (named as P-related defect state), and N-containing groups (named as N-related defect state) on sp^2 hybridized carbons of the synthesized CDs as shown in Figure 1ii [22]. Moreover, compared to the quantum dots and other organic dyes, the CDs usually exhibit large Stokes shifts. The QY of the CDs depends on the surface chemistry and preparation methods. Yellow-emissive CDs from anhydrous citric acid and 2,3-phenanzinediamine were prepared that exhibited large Stokes's shift (188 nm), excellent stability, and 24% quantum yield [53]. In another study, multi-color PL emissive CDs were synthesized from m-phenylenediamine (m-PD) and o-phenylenediamine (o-PD) and in the presence and absence of tartaric acid as the starting materials. Tartaric acid played a crucial role in tuning the surface state of CDs, such as the increase in surface oxidation and carboxylation. In the presence of tartaric acid (TA), the CDs from m-PD and o-PD exhibited green color and red color respectively whereas, in the absence of TA, CDs from m-PD and o-PD exhibited blue color and yellow-green color respectively. In particular, the red-CDs exhibited a high QY of up to 22.0%. [75]. The doping of CD changes the excitation-dependent PL. In a study, the emission of a bare CD that was found to be excitation-independent, showed a large red shift when it was doped with nitrogen. The reason is ascribed to the superimposition of blue (intrinsic molecular centers) and green emission bands (extrinsic molecular centers). In the emission process, the energy is transferred from the electron-hole pair formation at the intrinsic centers of the core to the extrinsic surface centers. Due to the surface defects and hybrid nanostructure in the mesoporous matrix, the contribution of the two bands modified, enhancing the tunability of the emission, thus promoting the green PL from blue emission. Besides, the QY of the CDs was found to vary, for the bare CDs (1.4%), N-doped CDs (22%), and purified N-CDs (28%) [76]. In another study by Kipnusu and co-researchers, nitrogen and boron doped carbon dots exhibited enhanced intersystem charge transfer (ICT) due to the presence of donor–acceptor moieties. Due to the ICT, the synthesized CDs produced triple color emission as shown in the Figure 1iii [39]. The properties of PL are controlled by the surface functionalization of CDs as well. Recently, surface functionalization was shown to enlarge and narrow the band gap energy. The fluorescence of

synthesized CDs could be quenched by tetracycline (TC) due to inner filter effect, whereas by introducing chlorotetracycline (CTC), blue-shift fluorescence was induced which may be due to enlarged energy band gap, and upon introducing oxytetracycline (OTC), fluorescence experienced red shift which could be because of the narrowed band gap as shown in Figure 1iv [15]. In a recent report, the addition of a long-alkyl chain to the CDs promoted the emission of white luminescence under UV light (365 nm), which may be due to the inhibition of the aggregation-caused quenching effect. Additionally, the alkyl chains can effectively interact with the lipophilic fatty residues that can increase the potential applications of the developed white-CDs [77]. Metal ion-dependent PL quenching of CDs has become a known phenomenon. In a report, the quenching mechanism has been identified as the photoinduced transfer of electrons from amine functional groups of the CDs to the respective metal ions [78].

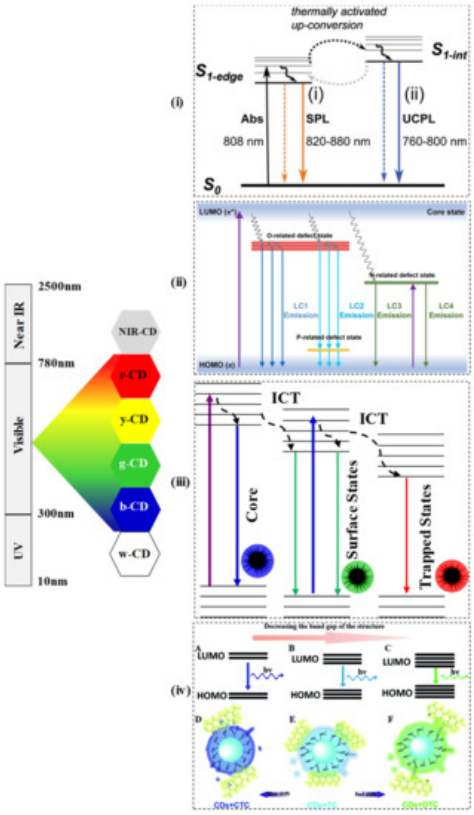

Figure 1. The band gap and transition of various color exhibited by CDs (near infrared CD: NIR-CD, red-CD: r-CD, yellow CD: y-CD, green CD: g-CD, blue CD: b-CD, white CD: w-CD). (**i**) Proposed mechanism of up-conversion PL in Near IR (NIR) CDs [74] (Reproduced with permission), (**ii**) Proposed mechanism of CDs with O-defects, P-defects and N-defects states [22] (Reproduced with permission). (**iii**) Energy diagram of the CDs indicating the role of intersystem, charge transfer [39] (Reproduced with permission). (**iv**) Band gap transitions of CDs by introducing CTC, TC, and OTC [15] (Reproduced with permission).

3.2.3. Electron Transfer of CDs

Typically, CDs can act as both an electron acceptor and donor. In an interesting study, considering the exceptional electron mobility property of the CDs at room temperature, CDs functionalized with ionic liquid were fabricated for their application as nanofluid in the field of energy. The nanofluids comprising of organic/inorganic hybrid systems could be used as electrolytes and separators for energy storage. Highly conductive Cdots, Cdots/[Bmim]Cl/[Tmi][Trif] and CdotsCHI/[Bmim]Cl/[Tmi][Trif], could be entrapped in poly(vinyl alcohol) membrane, which exhibited high proton conductivity. Moreover, the nanofluid's features remain constant for four months, even on wetting/drying cycles [79]. One of the most common applications of CDs is in the field of photocatalysis. The photocatalytic performance of the graphitic and amorphous CDs, which were synthesized using fructose, glucose, and citric acid, was investigated. In this study, the type of carbon source and the synthesis route that ultimately determines the potential of the photoelectron transfer determined the CD's structure and optical properties [80]. Pure carbonaceous CDs (without dopants) in graphitic form exhibited better photoactivity than the amorphous one, whereas, in the case of nitrogen-doped CDs, the amorphous CDs exhibited better photoredox-activity due to the presence of photo-active molecule. The graphitic defects and the dopant can quench each other, which reduces the photoactivity [81].

Heteroatom doping in carbon materials has long been used to create active catalytic sites and increases oxygen reduction reactions (ORR) in electrocatalysis. The performance of carbon-based catalysts, composites of doped CD and reduced graphene oxide (CD/rGO), and directly doped rGO were studied. In the finding, CD/rGO outperformed in ORR

measurement to their corresponding counterparts, and it is noted that N, S-co-doped too performed better than the individual doped N-CDs or S-CDs. Some of the reasons for such behaviour could be the synergistic effects of N, S-co-doping providing four-electron transfer pathways in ORR, active sites of on the CD surfaces and located at the edges/defects in abundant, which may have more accessibility to oxygen molecules. Another reason could be the effective components like graphitic N atoms and C-S-C/S-N species where current density and half-wave potential could be improved [82].

3.2.4. Cytotoxicity and Photostability of CDs

CDs are mostly known for their fascinating biocompatibility and relatively less toxicity, thus fulfilling the required conditions for diverse applications. The cytotoxicity of CDs, both in vitro and in vivo conditions, are extensively investigated. Moreover, CD's photostability is a crucial characteristic that can be explored for its efficient use as stable fluorescent probes. As the name suggests, photostability here means the labelled cell's fluorescence intensity remains stable for a considerable time. With this property, CDs are growingly used in cell imaging. Semi-conductor quantum dots were used in bioimaging methods because of their better photophysical properties than organic chromophores. The use of the conventional metal based QDs for biomedical applications are limited because of toxicity of the heavy metals like Pb and Cd, present in these nanomaterials. Since CDs are free from toxic heavy metals and possess high photostability, these are used in the bioimaging fields and medical diagnosis as well. However, a report of low toxicity of metal chelated CQD is available. A CQDs from citric acid and polyethylenimine was synthesised and covalently conjugated with 1,4,7,10-tetraazacyclononane (DOTA) to chelate lanthanide ion (Ln = Eu, Tb, Yb, and Gd). The CQDs-DOTA-Ln exhibited low cytotoxicity against Hela cells even at its high concentrations (500 µg/mL) [83]. However, the synthesis of metal-doped CDs is time-consuming, complicated, involves multiple steps, and requires post-synthetic treatments. In a recent development, ruthenium-containing CDs (Ru-CDs) were fabricated using a simple and efficient strategy. The developed CDs exhibited enhanced red fluorescence compared to the bare CD and Ru-complex and were employed as bioimaging agents for tumour cells and as photodynamic nanoagents for cancer therapy [84].

3.2.5. Emerging property: Chirality of CDs

More recently, efforts have also been made to develop chiral carbon dots for their application in a myriad of exciting areas ranging from sensing of chirality, separation of chiral molecules, chiral catalysis, bioimaging, and biomedicine. Among the two types of CD synthesis approaches, the "bottom-up" approach usually generates better chiral CDs as the precursor molecules themselves are chiral and therefore do not need the introduction of chiral ligands during the synthesis process [85]. A hybrid CD/CNC (cellulose nanocrystal) nanoparticle synthesized via hydrothermal route showed a dissymmetry factor of 0.2, which is higher than that of the reported dye/CNC hybrids. Furthermore, the nanoparticle displayed higher left-handed circularly polarized luminescence (CPL) emission than right-handed CPL emission. Based on the significant findings, these hybrids have a promising application to remove autofluorescence drawbacks in bioimaging. The CD/CNC hybrids can also be effectively employed in sensing, drug delivery, and photonic applications as mirror-free cholesteric lasers [86]. In another interesting study, using the concept of donor–acceptor complex formation between CDs and porphyrins, the chirality of the carbon nanodots was transferred to the porphyrin. This experimental finding provided the possibility of forming chiral composites for different applications [87]. In another approach to enhance the material property for biomedical applications, chiral CDs derived from glutamic acid were doped into gels as the latter display superior biocompatibility. An important aspect of such a doping process is the requirement of chiral match ability between the CD and the gelator, which would otherwise lead to the disintegration of the gel. It was shown that the doping of the chiral CD with the gelator (N,N-bis(octadecyl)-D-aminoglutamic diamide) to form gel resulted in the fluorescence enhancement of the CD. The enhancement was assumed to be the restriction of Brownian motion in the gel system that otherwise is responsible for decreased fluorescence intensity in the liquid system due to collisions between the CDs [88]. Fluorescence off-on sensors have an enormous demand for the development of smart monitoring systems. Using chiral CD synthesized from citric acid and L-aspartic acid, an on–off and off-on fluorescence sensor was developed to detect both Sn^{2+} ion and L-Lysine enantiomer. While the binding of Sn^{2+} on the surface of the CD resulted in fluorescence quenching (on-off), the addition of L-Lysine to the CD-Sn complex resulted in the enhancement of the fluorescence (off-on) as the L-Lysine preferentially has a stronger binding affinity for Sn^{2+} thereby recovery of the CD's fluorescence [89].

References

1. Maria Semeniuk; Zhihui Yi; Vida Poursorkhabi; Jimi Tjong; Shaffiq Jaffer; Zheng-Hong Lu; Mohini Sain; Future Perspectives and Review on Organic Carbon Dots in Electronic Applications. *ACS Nano* **2019**, *13*, 6224-6255, 10.1021/acsnano.9b00688.

2. Chao Hu; Mingyu Li; Jieshan Qiu; Ya-Ping Sun; Design and fabrication of carbon dots for energy conversion and storag e. *Chemical Society Reviews* **2019**, *48*, 2315-2337, 10.1039/c8cs00750k.

3. Jiyang Li; Bolun Wang; Hongyue Zhang; Jihong Yu; Carbon Dots-in-Matrix Boosting Intriguing Luminescence Propertie s and Applications. *Small* **2019**, *15*, e1805504, 10.1002/smll.201805504.

4. Pooja Devi; Prachi Rajput; Anupma Thakur; Ki-Hyun Kim; Praveen Kumar; Recent advances in carbon quantum dot-ba sed sensing of heavy metals in water. *TrAC Trends in Analytical Chemistry* **2019**, *114*, 171-195, 10.1016/j.trac.2019.03. 003.

5. Das, Smita; Goswami, Pranab. Nanozymes as Potential Catalysts for Sensing and Analytical Applications; Goswami, P ranab, Eds.; CRC press, Taylor & Francis group: Boca Raton, 2020; pp. 143-162.

6. Ngashangva, Lightson; Chakma, Babina; Goswami, Pranab. Smart Materials for Developing Sensor Platforms; Goswa mi, Pranab, Eds.; CRC press, Taylor & Francis group: Boca Raton, 2020; pp. 47-68.

7. Shoujun Zhu; Yubin Song; Xiaohuan Zhao; Jieren Shao; Junhu Zhang; Bai Yang; The photoluminescence mechanism i n carbon dots (graphene quantum dots, carbon nanodots, and polymer dots): current state and future perspective. *Nan o Research* **2015**, *8*, 355-381, 10.1007/s12274-014-0644-3.

8. Sadat Anwar; Haizhen Ding; Mingsheng Xu; Xiaolong Hu; Zhenzhen Li; Jingmin Wang; Li Liu; Lei Jiang; Dong Wang; C hen Dong; et al. Recent Advances in Synthesis, Optical Properties, and Biomedical Applications of Carbon Dots. *ACS Applied Bio Materials* **2019**, *2*, 2317-2338, 10.1021/acsabm.9b00112.

9. Zideng Gao; Shunyi Wang; Zijun Xu; Jin Liu; Yuanfang Huang; Shuwen Hu; Xueqin Ren; Synthesis of novel cationic ca rbon dots and application to quantitative detection of K+ in human serum samples. *New Journal of Chemistry* **2019**, *43*, 17937-17940, 10.1039/c9nj03990b.

10. Chuang He; Honghao Yan; Xiaojie Li; Xiaohong Wang; In situ fabrication of carbon dots-based lubricants using a facile ultrasonic approach. *Green Chemistry* **2019**, *21*, 2279-2285, 10.1039/c8gc04021d.

11. Wen-Bo Zhao; Kai-Kai Liu; Shi-Yu Song; Rui Zhou; Chong-Xin Shan; Fluorescent Nano-Biomass Dots: Ultrasonic-Assi sted Extraction and Their Application as Nanoprobe for Fe3+ detection. *Nanoscale Research Letters* **2019**, *14*, 1-9, 10. 1186/s11671-019-2950-x.

12. Vanthan Nguyen; Na Zhao; Lihe Yan; Peng Zhong; Van Canh Nguyen; Phuoc Huu Le; Double-pulse femtosecond laser ablation for synthesis of ultrasmall carbon nanodots. *Materials Research Express* **2019**, *7*, 015606, 10.1088/2053-159 1/ab6124.

13. Bin Chen; Shuiqin Chai; Jiahui Liu; Chuanjun Liu; Yanjie Li; Jiahui He; Zeping Yu; Tong Yang; Changhao Feng; Chengz hi Huang; et al. 2,4,6-Trinitrophenol detection by a new portable sensing gadget using carbon dots as a fluorescent pro be. *Analytical and Bioanalytical Chemistry* **2019**, *411*, 2291-2300, 10.1007/s00216-019-01670-z.

14. Roshni V.; Varsha Gujar; Heena Pathan; Sehbanul Islam; Madhumita Tawre; Karishma Pardesi; Manas Kumar Santra; Divya Ottoor; Bioimaging Applications of Carbon dots (C. dots) and its Cystamine Functionalization for the Sensitive De tection of Cr(VI) in Aqueous Samples. *Journal of Fluorescence* **2019**, *29*, 1381-1392, 10.1007/s10895-019-02448-3.

15. Hong Miao; Yingyi Wang; XiaoMing Yang; Carbon dots derived from tobacco for visually distinguishing and detecting th ree kinds of tetracyclines. *Nanoscale* **2018**, *10*, 8139-8145, 10.1039/c8nr02405g.

16. Chunsong Lu; Jie Liu; Lanlan Gan; XiaoMing Yang; Employing Cryptococcus-directed carbon dots for differentiating an d detecting m-benzenediol and p-benzenediol. *Sensors and Actuators B: Chemical* **2019**, *301*, 127077, 10.1016/j.snb.2 019.127077.

17. Lei Jiang; Haizhen Ding; Siyu Lu; Ting Geng; Guanjun Xiao; Bo Zou; Hong Bi; Photoactivated Fluorescence Enhancem ent in F,N-Doped Carbon Dots with Piezochromic Behavior. *Angewandte Chemie* **2019**, *132*, 10072-10077, 10.1002/an ge.201913800.

18. Anil Chandra; Neetu Singh; Cell Microenvironment pH Sensing in 3D Microgels Using Fluorescent Carbon Dots. *ACS B iomaterials Science & Engineering* **2017**, *3*, 3620-3627, 10.1021/acsbiomaterials.7b00740.

19. Yuanling Sun; Chaofan Ding; Yanna Lin; Weiyan Sun; Hao Liu; Xiaodong Zhu; Yuxue Dai; Chuannan Luo; Highly select ive and sensitive chemiluminescence biosensor for adenosine detection based on carbon quantum dots catalyzing lumi nescence released from aptamers functionalized graphene@magnetic β-cyclodextrin polymers. *Talanta* **2018**, *186*, 238 -247, 10.1016/j.talanta.2018.04.068.

20. Cheng He; Linkai Peng; Linzhe Lv; Yang Cao; Jinchun Tu; Wei Huang; Kexi Zhang; In situ growth of carbon dots on Ti O2 nanotube arrays for PEC enzyme biosensors with visible light response. *RSC Advances* **2019**, *9*, 15084-15091, 10. 1039/c9ra01045a.

21. Feng Huo; Ze Kang; Mingguang Zhu; Chao Tan; Yuran Tang; Yuhang Liu; Wei Zhang; Metal-triggered fluorescence enh ancement of multicolor carbon dots in sensing and bioimaging. *Optical Materials* **2019**, *94*, 363-370, 10.1016/j.optmat.2

019.06.012.

22. Pei Yang; Ziqi Zhu; Tao Zhang; Minzhi Chen; Yizhong Cao; Wei Zhang; Xin Wang; Xiaoyan Zhou; Weimin Chen; Facile synthesis and photoluminescence mechanism of green emitting xylose-derived carbon dots for anti-counterfeit printing. *Carbon* **2019**, *146*, 636-649, 10.1016/j.carbon.2019.02.028.

23. Shaomei Xu; Fangmei Zhang; Longbin Xu; Xin Liu; Pinyi Ma; Ying Sun; Xinghua Wang; DaQian Song; A fluorescence r esonance energy transfer biosensor based on carbon dots and gold nanoparticles for the detection of trypsin. *Sensors and Actuators B: Chemical* **2018**, *273*, 1015-1021, 10.1016/j.snb.2018.07.023.

24. Soheila Asadzadeh-Khaneghah; Aziz Habibi-Yangjeh; Kazuya Nakata; Decoration of carbon dots over hydrogen peroxi de treated graphitic carbon nitride: Exceptional photocatalytic performance in removal of different contaminants under v isible light. *Journal of Photochemistry and Photobiology A: Chemistry* **2019**, *374*, 161-172, 10.1016/j.jphotochem.2019. 02.002.

25. Mayank Pandey; Manoj Balachandran; Green Luminescence and Irradiance Properties of Carbon Dots Cross-linked wi th Polydimethylsiloxane. *The Journal of Physical Chemistry C* **2019**, *123*, 19835-19843, 10.1021/acs.jpcc.9b04130.

26. Min Pan; Zhen Xu; Qunying Jiang; Jie Feng; Junlin Sun; Fuan Wang; Xiaoqing Liu; Interfacial engineering of carbon do ts with benzenediboronic acid for fluorescent biosensing. *Nanoscale Advances* **2018**, *1*, 765-771, 10.1039/c8na00166 a.

27. Yifang Gao; Yuan Jiao; Wenjing Lu; Yang Liu; Hui Han; Xiaojuan Gong; Ming Xian; Shaomin Shuang; Chuan Dong; Ca rbon dots with red emission as a fluorescent and colorimeteric dual-readout probe for the detection of chromium(vi) and cysteine and its logic gate operation. *Journal of Materials Chemistry B* **2018**, *6*, 6099-6107, 10.1039/c8tb01580e.

28. Guoliang Liu; Da-Qian Feng; Yanling Qian; Wei Wang; Jun-Jie Zhu; Construction of FRET biosensor for off-on detectio n of lead ions based on carbon dots and gold nanorods.. *Talanta* **2019**, *201*, 90-95, 10.1016/j.talanta.2019.03.101.

29. Benjamin P. Frank; Leslie R. Sigmon; Alyssa R. Deline; Ronald S. Lankone; Miranda J. Gallagher; Bo Zhi; Christy L. Ha ynes; D. Howard Fairbrother; Photochemical Transformations of Carbon Dots in Aqueous Environments. *Environmental Science & Technology* **2020**, *54*, 4160-4170, 10.1021/acs.est.9b07437.

30. Julian Schneider; Claas J. Reckmeier; Yuan Xiong; Maximilian Von Seckendorff; Andrei S. Susha; Peter Kasák; Andrey L. Rogach; Molecular Fluorescence in Citric Acid-Based Carbon Dots. *The Journal of Physical Chemistry C* **2017**, *121*, 2014-2022, 10.1021/acs.jpcc.6b12519.

31. Shoujun Zhu; Xiaohuan Zhao; Yubin Song; Siyu Lu; Bai Yang; Beyond bottom-up carbon nanodots: Citric-acid derived organic molecules. *Nano Today* **2016**, *11*, 128-132, 10.1016/j.nantod.2015.09.002.

32. Bo Ju; Hui Nie; Xiao-Guang Zhang; Qiaonan Chen; Xiaowei Guo; Zhen Xing; Minjie Li; Sean Xiao-An Zhang; Inorganic Salt Incorporated Solvothermal Synthesis of Multicolor Carbon Dots, Emission Mechanism, and Antibacterial Study. *AC S Applied Nano Materials* **2018**, *1*, 6131-6138, 10.1021/acsanm.8b01355.

33. Rajkumar Bandi; Ramakrishna Dadigala; Bhagavanth Reddy Gangapuram; Veerabhadram Guttena; Green synthesis o f highly fluorescent nitrogen – Doped carbon dots from Lantana camara berries for effective detection of lead(II) and bio imaging. *Journal of Photochemistry and Photobiology B: Biology* **2018**, *178*, 330-338, 10.1016/j.jphotobiol.2017.11.010.

34. Bedia Begüm Karakoçak; Jue Liang; Shalinee Kavadiya; Mikhail Y. Berezin; Pratim Biswas; Nathan Ravi; Optimizing th e Synthesis of Red-Emissive Nitrogen-Doped Carbon Dots for Use in Bioimaging. *ACS Applied Nano Materials* **2018**, *1*, 3682-3692, 10.1021/acsanm.8b00799.

35. Theodoros Chatzimitakos; Athanasia Kasouni; Lamprini Sygellou; Ioannis Leonardos; Anastasios Troganis; Constantin e Stalikas; Human fingernails as an intriguing precursor for the synthesis of nitrogen and sulfur-doped carbon dots with strong fluorescent properties: Analytical and bioimaging applications. *Sensors and Actuators B: Chemical* **2018**, *267*, 4 94-501, 10.1016/j.snb.2018.04.059.

36. Yan Duan; Yijun Huang; Shengyu Chen; Weiyuan Zuo; Bingfang Shi; Cu-Doped Carbon Dots as Catalysts for the Che miluminescence Detection of Glucose. *ACS Omega* **2019**, *4*, 9911-9917, 10.1021/acsomega.9b00738.

37. Quan Xu; Rigu Su; Yusheng Chen; Sreeprasad Theruvakkattil Sreenivasan; Neng Li; Xusheng Zheng; Junfa Zhu; Haibi n Pan; Weijun Li; Chunming Xu; et al. Metal Charge Transfer Doped Carbon Dots with Reversibly Switchable, Ultra-Hig h Quantum Yield Photoluminescence. *ACS Applied Nano Materials* **2018**, *1*, 1886-1893, 10.1021/acsanm.8b00277.

38. I.C. Novoa-De León; J. Johny; S. Vázquez-Rodríguez; N. García-Gómez; S. Carranza-Bernal; I. Mendivil; S. Shaji; S. S epúlveda-Guzmán; Tuning the luminescence of nitrogen-doped graphene quantum dots synthesized by pulsed laser ab lation in liquid and their use as a selective photoluminescence on–off–on probe for ascorbic acid detection. *Carbon* **201 9**, *150*, 455-464, 10.1016/j.carbon.2019.05.057.

39. Wycliffe Kiprop Kipnusu; Carlos Doñate-Buendía; Mercedes Fernández-Alonso; Jesús Lancis; Gladys Mínguez-Vega; Nonlinear Optics to Glucose Sensing: Multifunctional Nitrogen and Boron Doped Carbon Dots with Solid-State Fluoresc

ence in Nanoporous Silica Films. *Particle & Particle Systems Characterization* **2020**, *37*, 2000093, 10.1002/ppsc.202000093.

40. Yiyang Wu; Youdi Liu; Jingya Yin; Haitao Li; Jun Huang; Facile ultrasonic synthesized NH2-carbon quantum dots for ultrasensitive Co2+ ion detection and cell imaging. *Talanta* **2019**, *205*, 120121, 10.1016/j.talanta.2019.120121.

41. Xiaohong Chu; Fan Wu; Baohong Sun; Ming Zhang; Saijie Song; Pan Zhang; Yuli Wang; Qicheng Zhang; Ninglin Zhou; Jian Shen; et al. Genipin cross-linked carbon dots for antimicrobial, bioimaging and bacterial discrimination. *Colloids and Surfaces B: Biointerfaces* **2020**, *190*, 110930, 10.1016/j.colsurfb.2020.110930.

42. Raji Atchudan; Thomas Nesakumar Jebakumar Immanuel Edison; Suguna Perumal; N. Clament Sagaya Selvam; Yong Rok Lee; Green synthesized multiple fluorescent nitrogen-doped carbon quantum dots as an efficient label-free optical nanoprobe for in vivo live-cell imaging. *Journal of Photochemistry and Photobiology A: Chemistry* **2019**, *372*, 99-107, 10.1016/j.jphotochem.2018.12.011.

43. Ivana Milenkovic; Manuel Algarra; Cristina Alcoholado; Manuel Cifuentes; Juan M. Lázaro-Martínez; Enrique Rodríguez-Castellón; Dragosav Mutavdžić; Ksenija Radotić; Teresa J. Bandosz; Fingerprint imaging using N-doped carbon dots. *Carbon* **2019**, *144*, 791-797, 10.1016/j.carbon.2018.12.102.

44. Jing Fang; Shujuan Zhuo; Changqing Zhu; Fluorescent sensing platform for the detection of p-nitrophenol based on Cu-doped carbon dots. *Optical Materials* **2019**, *97*, 109396, 10.1016/j.optmat.2019.109396.

45. Tianyi Zhanga; Si Donga; Feifei Zhaoa; Mingxiao Denga; Yuqin Fub; Changli Lüa; Tricolor emissive carbon dots for ultra-wide range pH test papers and bioimaging. *Sensors and Actuators B: Chemical* **2019**, *298*, 126869, 10.1016/j.snb.2019.126869.

46. Nan Wang; Mengke Wang; Yang Yu; Guojian Yang; Xingguang Su; Label-free fluorescence assay based on near-infrared B,N-doped carbon dots as a fluorescent probe for the detection of sialic acid. *New Journal of Chemistry* **2020**, *44*, 2350-2356, 10.1039/c9nj05981d.

47. Chunmei Li; Zhaojian Qin; Maonan Wang; Weiwei Liu; Hui Jiang; Xuemei Wang; Manganese oxide doped carbon dots for temperature-responsive biosensing and target bioimaging. *Analytica Chimica Acta* **2020**, *1104*, 125-131, 10.1016/j.aca.2020.01.001.

48. Indrajit Srivastava; Santosh K. Misra; Sushant Bangru; Kingsley A. Boateng; Julio A. N. T. Soares; Aaron S. Schwartz-Duval; Auinash Kalsotra; Dipanjan Pan; Complementary Oligonucleotide Conjugated Multicolor Carbon Dots for Intracellular Recognition of Biological Events. *ACS Applied Materials & Interfaces* **2020**, *12*, 16137-16149, 10.1021/acsami.0c02463.

49. Somen Mondal; Anna Yucknovsky; Katherine Akulov; Nandan Ghorai; Tal Schwartz; Hirendra N. Ghosh; Nadav Amdursky; Efficient Photosensitizing Capabilities and Ultrafast Carrier Dynamics of Doped Carbon Dots. *Journal of the American Chemical Society* **2019**, *141*, 15413-15422, 10.1021/jacs.9b08071.

50. Yuan-Yuan Ding; Xiao-Juan Gong; Yang Liu; Wen-Jing Lu; Yi-Fang Gao; Ming Xian; Shao-Min Shuang; Chuan Dong; Facile preparation of bright orange fluorescent carbon dots and the constructed biosensing platform for the detection of pH in living cells. *Talanta* **2018**, *189*, 8-15, 10.1016/j.talanta.2018.06.060.

51. Cheng-Long Shen; Jin-Hao Zang; Qing Lou; Li-Xia Su; Zhen Li; Zhi-Yu Liu; Lin Dong; Chong-Xin Shan; In-situ embedding of carbon dots in a trisodium citrate crystal matrix for tunable solid-state fluorescence. *Carbon* **2018**, *136*, 359-368, 10.1016/j.carbon.2018.05.015.

52. Yan Zhan; Ting Geng; Yingliang Liu; Chaofan Hu; Xuejie Zhang; Bingfu Lei; Jianle Zhuang; Xu Wu; Di Huang; Guanjun Xiao; et al. Near-Ultraviolet to Near-Infrared Fluorescent Nitrogen-Doped Carbon Dots with Two-Photon and Piezochromic Luminescence. *ACS Applied Materials & Interfaces* **2018**, *10*, 27920-27927, 10.1021/acsami.8b07498.

53. Fanyong Yan; Zhangjun Bai; Fanlin Zu; Yan Zhang; Xiaodong Sun; Tengchuang Ma; Liang Chen; Yellow-emissive carbon dots with a large Stokes shift are viable fluorescent probes for detection and cellular imaging of silver ions and glutathione. *Microchimica Acta* **2019**, *186*, 113, 10.1007/s00604-018-3221-8.

54. Fanglong Yuan; Ya-Kun Wang; Geetu Sharma; Yitong Dong; Xiaopeng Zheng; Peicheng Li; Andrew Johnston; Golam Bappi; James Z. Fan; Hao Kung; et al. Bright high-colour-purity deep-blue carbon dot light-emitting diodes via efficient edge amination. *Nature Photonics* **2019**, *14*, 171-176, 10.1038/s41566-019-0557-5.

55. Jingmin Wang; Mingsheng Xu; Dong Wang; Zhenzhen Li; Fernando Lucas Primo; Antonio Claudio Tedesco; Hong Bi; Copper-Doped Carbon Dots for Optical Bioimaging and Photodynamic Therapy. *Inorganic Chemistry* **2019**, *58*, 13394-13402, 10.1021/acs.inorgchem.9b02283.

56. Chaoge Cheng; Malcolm Xing; Qilin Wu; A universal facile synthesis of nitrogen and sulfur co-doped carbon dots from cellulose-based biowaste for fluorescent detection of Fe3+ ions and intracellular bioimaging. *Materials Science and Engineering: C* **2019**, *99*, 611-619, 10.1016/j.msec.2019.02.003.

57. Zhao Mu; Jianhao Hua; Shouai Feng; Yaling Yang; A ratiometric fluorescence and light scattering sensing platform bas ed on Cu-doped carbon dots for tryptophan and Fe(III).. *Spectrochimica Acta Part A: Molecular and Biomolecular Spect roscopy* **2019**, *219*, 248-256, 10.1016/j.saa.2019.04.065.

58. Linbo Li; Tao Dong; Photoluminescence tuning in carbon dots: surface passivation or/and functionalization, heteroatom doping. *Journal of Materials Chemistry C* **2018**, *6*, 7944-7970, 10.1039/c7tc05878k.

59. Yuting Bai; Bai Zhang; Lu Chen; Zhenjie Lin; Xiuming Zhang; Dongtao Ge; Wei Shi; Yanan Sun; Facile One-Pot Synthe sis of Polydopamine Carbon Dots for Photothermal Therapy.. *Nanoscale Research Letters* **2018**, *13*, 287, 10.1186/s11 671-018-2711-2.

60. K. Radhakrishnan; P. Panneerselvam; M. Marieeswaran; Radhakrishnan Kothalam; Panneerselvam Perumal; Mariees waran Muppidathi; A green synthetic route for the surface-passivation of carbon dots as an effective multifunctional fluo rescent sensor for the recognition and detection of toxic metal ions from aqueous solution. *Analytical Methods* **2018**, *1 1*, 490-506, 10.1039/c8ay02451k.

61. Rebecca Momper; Julian Steinbrecher; Matthias Dorn; Irina Rörich; Simon Bretschneider; Manuel Tonigold; Charushee la Ramanan; Sandra Ritz; Volker Mailänder; Katharina Landfester; et al. Enhanced photoluminescence properties of a carbon dot system through surface interaction with polymeric nanoparticles. *Journal of Colloid and Interface Science* **2 018**, *518*, 11-20, 10.1016/j.jcis.2018.01.102.

62. Mingxi Yang; Qiuling Tang; Yang Meng; Junjun Liu; Tanglue Feng; Xiaohuan Zhao; Shoujun Zhu; Weixian Yu; Bai Yang; Reversible “Off–On” Fluorescence of Zn2+-Passivated Carbon Dots: Mechanism and Potential for the Detection of ED TA and Zn2+. *Langmuir* **2018**, *34*, 7767-7775, 10.1021/acs.langmuir.8b00947.

63. Xinyue Rao; Mengke Yuan; Huan Jiang; Ling Li; Zhongde Liu; A universal strategy to obtain chiroptical carbon quantum dots through the optically active surface passivation procedure. *New Journal of Chemistry* **2019**, *43*, 13735-13740, 10. 1039/c9nj03434j.

64. Gui-Hua Yan; Zheng-Mei Song; Yuan-Yuan Liu; Qianqian Su; Weixiong Liang; Aoneng Cao; Ya-Ping Sun; Haifang Wan g; Effects of carbon dots surface functionalities on cellular behaviors – Mechanistic exploration for opportunities in mani pulating uptake and translocation. *Colloids and Surfaces B: Biointerfaces* **2019**, *181*, 48-57, 10.1016/j.colsurfb.2019.05. 027.

65. Qingnan Zhao; Wei Song; Bing Zhao; Bai Yang; Spectroscopic studies of the optical properties of carbon dots: recent a dvances and future prospects. *Materials Chemistry Frontiers* **2019**, *4*, 472-488, 10.1039/c9qm00592g.

66. Quan Xu; Weijun Li; Lan Ding; Wenjing Yang; Haihua Xiao; Wee-Jun Ong; Function-driven engineering of 1D carbon n anotubes and 0D carbon dots: mechanism, properties and applications. *Nanoscale* **2018**, *11*, 1475-1504, 10.1039/c8nr 08738e.

67. Jelinek, R. Characterization and Physical Properties of Carbon-Dots; Jelinek, R, Eds.; Springer International Publishin g: Switzerland, 2017; pp. 29-46.

68. Zhenhui Kang; Shuit-Tong Lee; Carbon dots: advances in nanocarbon applications. *Nanoscale* **2019**, *11*, 19214-19224, 10.1039/c9nr05647e.

69. Xiao Wang; Yongqiang Feng; Peipei Dong; Jianfeng Huang; A Mini Review on Carbon Quantum Dots: Preparation, Pro perties, and Electrocatalytic Application. *Frontiers in Chemistry* **2019**, *7*, 671, 10.3389/fchem.2019.00671.

70. Somayeh Tajik; Zahra Dourandish; Kaiqiang Zhang; Hadi Beitollahi; Quyet Van Le; Ho Won Jang; Mohammadreza Sho kouhimehr; Carbon and graphene quantum dots: a review on syntheses, characterization, biological and sensing applic ations for neurotransmitter determination. *RSC Advances* **2020**, *10*, 15406-15429, 10.1039/d0ra00799d.

71. Abu Bakar Siddique; Ashit Kumar Pramanick; Subrata Chatterjee; Mallar Ray; Amorphous Carbon Dots and their Rema rkable Ability to Detect 2,4,6-Trinitrophenol. *Scientific Reports* **2018**, *8*, 9770, 10.1038/s41598-018-28021-9.

72. Syamantak Khan; Navneet C. Verma; Chethana; Chayan K. Nandi; Carbon Dots for Single-Molecule Imaging of the Nu cleolus. *ACS Applied Nano Materials* **2018**, *1*, 483-487, 10.1021/acsanm.7b00175.

73. Wenjuan Dong; Ruiping Wang; Xiaojuan Gong; Chuan Dong; An efficient turn-on fluorescence biosensor for the detecti on of glutathione based on FRET between N,S dual-doped carbon dots and gold nanoparticles. *Analytical and Bioanaly tical Chemistry* **2019**, *411*, 6687-6695, 10.1007/s00216-019-02042-3.

74. Di Li; Chao Liang; Elena V. Ushakova; Minghong Sun; Xiaodan Huang; Xiaoyu Zhang; Pengtao Jing; Seung Jo Yoo; Ji n-Gyu Kim; Enshan Liu; et al. Thermally Activated Upconversion Near-Infrared Photoluminescence from Carbon Dots S ynthesized via Microwave Assisted Exfoliation. *Small* **2019**, *15*, e1905050, 10.1002/smll.201905050.

75. Kai Jiang; Xiangyu Feng; Xiaolu Gao; Yuhui Wang; Congzhong Cai; Zhongjun Li; Hengwei Lin; Preparation of Multicolo r Photoluminescent Carbon Dots by Tuning Surface States. *Nanomaterials* **2019**, *9*, 529, 10.3390/nano9040529.

76. Carlo Maria Carbonaro; Daniele Chiriu; Luigi Stagi; Maria Francesca Casula; Swapneel V. Thakkar; Luca Malfatti; Kazu masa Suzuki; Pier Carlo Ricci; Riccardo Corpino; Carbon Dots in Water and Mesoporous Matrix: Chasing the Origin of their Photoluminescence. *The Journal of Physical Chemistry C* **2018**, *122*, 25638-25650, 10.1021/acs.jpcc.8b08012.
77. Bang-Ping Jiang; Yun-Xiang Yu; Xiao-Lu Guo; Zhao-Yang Ding; Bo Zhou; Hong Liang; Xing-Can Shen; White-emitting carbon dots with long alkyl-chain structure: Effective inhibition of aggregation caused quenching effect for label-free im aging of latent fingerprint. *Carbon* **2018**, *128*, 12-20, 10.1016/j.carbon.2017.11.070.
78. Keenan J. Mintz; Brenda Guerrero; Roger M. Leblanc; Photoinduced Electron Transfer in Carbon Dots with Long-Wave length Photoluminescence. *The Journal of Physical Chemistry C* **2018**, *122*, 29507-29515, 10.1021/acs.jpcc.8b06868.
79. Helena M. R. Gonçalves; Susana A. F. Neves; Abel Duarte; Verónica De Zea Bermudez; Nanofluid Based on Carbon D ots Functionalized with Ionic Liquids for Energy Applications. *Energies* **2020**, *13*, 649, 10.3390/en13030649.
80. Amadio Emanuele; Simone Cailotto; Carlotta Campalani; Lorenzo Branzi; Carlotta Raviola; Davide Ravelli; Elti Cattaru zza; Enrico Trave; Alvise Benedetti; Maurizio Selva; et al. Precursor-Dependent Photocatalytic Activity of Carbon Dots. *Molecules* **2019**, *25*, 101, 10.3390/molecules25010101.
81. Simone Cailotto; Raffaello Mazzaro; Francesco Enrichi; Alberto Vomiero; Maurizio Selva; Elti Cattaruzza; Davide Cristo fori; Emanuele Amadio; Alvise Perosa; Design of Carbon Dots for Metal-free Photoredox Catalysis. *ACS Applied Materi als & Interfaces* **2018**, *10*, 40560-40567, 10.1021/acsami.8b14188.
82. Peng Zhang; Ji-Shi Wei; Xiao-Bo Chen; Huan-Ming Xiong; Heteroatom-doped carbon dots based catalysts for oxygen r eduction reactions. *Journal of Colloid and Interface Science* **2019**, *537*, 716-724, 10.1016/j.jcis.2018.11.024.
83. Fengshou Wu; Liangliang Yue; Lixia Yang; Kai Wang; Genyan Liu; Xiaogang Luo; Xunjin Zhu; Ln(III) chelates-functiona lized carbon quantum dots: Synthesis, optical studies and multimodal bioimaging applications. *Colloids and Surfaces B: Biointerfaces* **2019**, *175*, 272-280, 10.1016/j.colsurfb.2018.11.054.
84. Liangliang Yue; Haolan Li; Qi Sun; Juan Zhang; Xiaogang Luo; Fengshou Wu; Xunjin Zhu; Red-Emissive Ruthenium-C ontaining Carbon Dots for Bioimaging and Photodynamic Cancer Therapy. *ACS Applied Nano Materials* **2019**, *3*, 869-8 76, 10.1021/acsanm.9b02394.
85. Yi Ru; Lin Ai; Tongtong Jia; Xingjiang Liu; Siyu Lu; Zhiyong Tang; Bai Yang; Recent advances in chiral carbonized poly mer dots: From synthesis and properties to applications. *Nano Today* **2020**, *34*, 100953, 10.1016/j.nantod.2020.10095 3.
86. Mahshid Chekini; Elisabeth Prince; Lily Zhao; Haridas Mundoor; Ivan I. Smalyukh; Eugenia Kumacheva; Chiral Carbon Dots Synthesized on Cellulose Nanocrystals. *Advanced Optical Materials* **2019**, *8*, 1901911, 10.1002/adom.20190191 1.
87. Luka Đorđević; Francesca Arcudi; Alessandro D'Urso; Michele Cacioppo; Norberto Micali; Thomas Bürgi; Roberto Purr ello; Maurizio Prato; Design principles of chiral carbon nanodots help convey chirality from molecular to nanoscale leve l. *Nature Communications* **2018**, *9*, 1-8, 10.1038/s41467-018-05561-2.
88. Lulu Zhou; Dongxiao Zheng; Bin Wu; Yiqing Zhu; Liangliang Zhu; Gel Systems Doped with Chiral Carbon Dots for Opti cal Combination. *ACS Applied Nano Materials* **2019**, *3*, 946-952, 10.1021/acsanm.9b01677.
89. Pengli Gao; Zhigang Xie; Min Zheng; Chiral carbon dots-based nanosensors for Sn(II) detection and lysine enantiomer s recognition. *Sensors and Actuators B: Chemical* **2020**, *319*, 128265, 10.1016/j.snb.2020.128265.
90. Pengli Gao; Zhigang Xie; Min Zheng; Chiral carbon dots-based nanosensors for Sn(II) detection and lysine enantiomer s recognition. *Sensors and Actuators B: Chemical* **2020**, *319*, 128265, 10.1016/j.snb.2020.128265.
